Fermi Surface and Effective Mass in Doped GaSb†

H. I. ZHANG*
Department of Physics, Louisiana State University, Baton Rouge, Louisiana 70803
(Received 16 June 1969)

An analytic representation has been obtained for the conduction band and valence bands near $\mathbf{k}=0$ for GaSb. The periods of the magnetoresistance oscillations are calculated as functions of the Fermi energy for the three magnetic field directions: ⟨100⟩, ⟨110⟩, and ⟨111⟩. The Fermi-level dependence and the anisotropy of the periods are in excellent agreement with experiment. The beating effect due to the inversion asymmetry splitting is estimated. The effective masses for the conduction, heavy-hole, light-hole, and split-off bands are evaluated as functions of Fermi energy in the three major directions. The carrier-concentration dependence of the effective mass is obtained for the conduction band. The calculated Fermi energy dependence and anisotropy of the effective masses are compared with experiment.

I. INTRODUCTION

THE shape of the Fermi surface for n-type GaSb has been intensively investigated since the oscillations in the magnetoresistance (the Shubnikov–de Haas effect) were first observed by Becker and Fan[1] for this material. Yep and Becker[2] measured the periods of oscillations in the Hall coefficient and magnetoresistance for a number of samples with different Fermi levels. Seiler and Becker[3] observed the beating patterns in the Shubnikov–de Haas oscillations in GaSb which are similar to those observed by Whitsett[4] in HgSe. These patterns were interpreted as arising from the inversion asymmetry splitting by Roth *et al.*[5] More recently, Seiler and Becker[6] measured the frequencies of the Shubnikov–de Haas oscillations with the magnetic field in a number of different directions and obtained a remarkable anisotropy. They also estimated the anisotropy in the conduction-band effective mass.

The dependence of the conduction-band effective mass upon the carrier concentration has been investigated for many III-V compounds. Palik and Wright[7] provided a summary of a large number of experimental results which show that the carrier-concentration dependence of the effective mass in these materials is quite significant. In InSb, for example, the value of the effective mass measured for a sample with carrier concentration $\sim 10^{18}$ cm^{-3} is about three times as large as the corresponding value for a sample with carrier concentration $\sim 10^{15}$ cm^{-3}. For GaSb, Yep and Becker[8] obtained the conduction-band effective masses for a set of samples with different degrees of carrier concentration by analyzing the measured Shubnikov–de Haas oscillations. In addition to reporting their own results, they provided a summary of the values obtained by other investigators with different methods and samples.

The Fermi surface and effective mass in p-type GaSb, which correspond to the valence-band structure of the material, has been less extensively investigated. Stradling[9] measured the cyclotron-resonance effective masses for the heavy-hole and light-hole bands for the three major directions of magnetic field. He observed a strong anisotropy in heavy-hole mass.

It is desirable to have a consistent theoretical explanation for the experimental data with regard to the Fermi surface and effective mass in doped GaSb. Previously, most of the theoretical explanations have been based on the $\mathbf{k}\cdot\mathbf{p}$ theory of Kane.[10] Kołodziejczak *et al.*,[11] in particular, calculated the carrier-concentration dependence of the effective masses for a large number of III-V compounds using $\mathbf{k}\cdot\mathbf{p}$ theory and experimentally obtained band parameters.

In the present paper, we report the result of an analysis of the energy-band shape near $\mathbf{k}=0$, which is based on a previous band calculation for this material.[12] An analytic representation of the energy band near $\mathbf{k}=0$ is obtained by expanding the energy in terms of Kubic harmonics for each band and determining the coefficients using a least-squares procedure. The extremal cross-sectional areas and their derivatives with regard to the Fermi levels are evaluated in the three major symmetry directions: ⟨100⟩, ⟨110⟩, and ⟨111⟩. This gives the Fermi-level dependence and anisotropy of the frequencies of Shubnikov–de Haas oscillations and effective masses for the material. The carrier-concentration dependence of the effective mass is evaluated

† Work supported by the U. S. Air Force Office of Scientific Research under Grant No. AFOSR 68-1565.
* Present address: Department of Physics, University of Texas, Austin, Tex. 78712.
[1] W. M. Becker and H. Y. Fan, in *Proceedings of the International Conference on the Physics of Semiconductors, Paris, 1964* (Dunod Cie., Paris, 1964), p. 663.
[2] T. O. Yep and W. M. Becker, Phys. Rev. **156**, 939 (1967).
[3] D. G. Seiler and W. M. Becker, Phys. Letters **26A**, 96 (1967).
[4] C. R. Whitsett, Phys. Rev. **138**, A829 (1965).
[5] L. M. Roth, S. H. Groves, and P. W. Wyatt, Phys. Rev. Letters **19**, 576 (1967); L. M. Roth, Phys. Rev. **173**, 755 (1968).
[6] D. G. Seiler and W. M. Becker, Phys. Rev. **183**, 784 (1969).
[7] E. D. Palik and G. B. Wright, in *Semiconductors and Semimetals*, edited by R. K. Willardson and A. C. Beer (Academic Press Inc., New York, 1967), Vol. 3, p. 421.
[8] T. O. Yep and W. M. Becker, Phys. Rev. **144**, 741 (1966).
[9] R. A. Stradling, Phys. Letters **20**, 217 (1966).
[10] E. O. Kane, J. Phys. Chem. Solids **1**, 83 (1956); E. O. Kane, in *Semiconductors and Semimetals*, edited by R. K. Willardson and A. C. Beer (Academic Press Inc., New York, 1966), Vol. 1, p. 75.
[11] J. Kołodziejczak, S. Zukotyński, and H. Stramska, Phys. Status Solidi **14**, 471 (1966); J. Kołodziejczak and S. Zukotyński, *ibid.* **16**, K55 (1966).
[12] H. I. Zhang and J. Callaway, Phys. Rev. **181**, 1163 (1969).

explicitly for the conduction band. An estimate for the distance between two successive nodes is made by evaluating the difference between two extremal cross-sectional areas split due to the inversion asymmetry. Comparisons with the corresponding experimental values are made for all the results if such are available.

The present work differs from most of the previous theoretical investigations in that the present results are obtained directly from the calculated energy bands, while most of the previous calculations on this subject were performed in $\mathbf{k}\cdot\mathbf{p}$ theory using some experimentally obtained band parameters and thus not related to any particular energy-band calculation.

II. ENERGY-BAND REPRESENTATION

In a previous work,[12] we have determined a pseudo-Hamiltonian and calculated the energy bands of GaSb, which reproduced most of the important band characteristics in a remarkable precision. From this calculation, we can obtain the energy levels for a given point in the reciprocal space by diagonalizing the Hamiltonian matrix. However, in order to determine the Fermi surface and effective mass as functions of the Fermi energy, it is necessary to obtain an analytical representation of the energy band $E(\mathbf{k})$ in the space of the wave vector $\mathbf{k}$.

An energy band $E(\mathbf{k})$ in $\mathbf{k}$ space possesses the point group symmetry of the crystal and also the inversion symmetry

$$E(\mathbf{k})=E(-\mathbf{k})$$

due to the time reversal symmetry of Hamiltonian. This is also true for the energy bands which are obtained from a Hamiltonian including spin-orbit interaction. Since an energy band is a scalar in $\mathbf{k}$ space, it possesses Γ_1 symmetry in cubic crystals. A nondegenerate band is assumed to be analytic (regular) in $\mathbf{k}$ space throughout the Brillouin zone[13] and therefore can be expanded in terms of polynomials of k_x, k_y, and k_z. Using the symmetry property of $E(\mathbf{k})$, we can expand a nondegenerate band in Kubic harmonics as

$$E(\mathbf{k})=E_0+E_2k^2+(E_4^{(1)}+E_4^{(2)}K_{4,1})k^4 +(E_6^{(1)}+E_6^{(2)}K_{4,1}+E_6^{(3)}K_{6,1})k^6+\cdots, \quad (2.1)$$

where the Kubic harmonics $K_{4,1}$ and $K_{6,1}$ are given by[14]

$$K_{4,1}=\frac{5}{4}(21)^{1/2}\left(\frac{k_x^4+k_y^4+k_z^4}{k^4}-\frac{3}{5}\right), \quad (2.2)$$

$$K_{6,1}=\left(\frac{639639}{32}\right)^{1/2}\left[\frac{k_x^2k_y^2k_z^2}{k^6} +\frac{1}{22}\left(\frac{k_x^4+k_y^4+k_z^4}{k^4}-\frac{3}{5}\right)-\frac{1}{105}\right]. \quad (2.3)$$

Callaway[15] has used this expansion for the analysis of the lithium band structure.

The valence bands, which are degenerate at $\mathbf{k}=0$, may not adequately be approximated by the above expansion due to the nonanalyticity at the point of degeneracy. Without spin-orbit coupling, the valence bands near $\mathbf{k}=0$ are determined by $\mathbf{k}\cdot\mathbf{p}$ perturbation theory as solutions of the secular equation[16]

$$\begin{vmatrix} Lk_x^2+M(k_y^2+k_z^2)-E & Nk_xk_y & Nk_xk_z \\ Nk_xk_y & Lk_y^2+M(k_x^2+k_z^2)-E & Nk_yk_z \\ Nk_xk_z & Nk_yk_z & Lk_z^2+M(k_x^2+k_y^2)-E \end{vmatrix}=0. \quad (2.4)$$

The quantities L, M, and N are sums of certain matrix elements. It is obvious that the solution of (2.4), in general, may give rise to second-order anisotropic terms in $\mathbf{k}$ space.

If we include the spin-orbit coupling effect, all the bands are regarded to be at least doubly degenerate at $\mathbf{k}=0$ and along some symmetry axes. (For a crystal with inversion symmetry, however, we can ignore this double degeneracy because the degeneracy is not lifted anywhere in the Brillouin zone.) Therefore, even the conduction band and split-off valence band, which can be regarded as nondegenerate if we neglect the inversion asymmetry splitting, cannot adequately be represented by (2.1).

On the other hand, the shape of the energy band around $\mathbf{k}=0$ can be analyzed by $\mathbf{k}\cdot\mathbf{p}$ perturbation theory. For small $\mathbf{k}$, the band, including spin-orbit coupling effects, has been given by the three-band approximation of Kane[10] in the form

$$E(\mathbf{k})^{\pm}=E_0+(E_2^{(1)}+E_2^{(2)}T_2)k^2\pm E_3T_3k^3, \quad (2.5)$$

where

$$T_2=(1/k^4)(k_x^2k_y^2+k_y^2k_z^2+k_z^2k_x^2) \quad (2.6)$$

and

$$T_3=(1/k^3)[k^2(k_x^2k_y^2+k_y^2k_z^2+k_z^2k_x^2) -9k_x^2k_y^2k_z^2]^{1/2}. \quad (2.7)$$

In (2.5), the constant $E_2^{(2)}$ vanishes for the conduction and split-off bands. For the heavy-hole band, the term containing T_3 is absent. We here observe that the term

[13] W. Kohn, Phys. Rev. 115, 809 (1959). Kohn proved the analyticity of the nondegerate band for one-dimensional solids. We assume that this is also true for three-dimensional solids.

[14] F. C. Von der Lage and H. A. Bethe, Phys. Rev. 71, 612 (1947).

[15] J. Callaway, Phys. Rev. 124, 1824 (1961).

[16] G. Dresselhaus, A. F. Kip, and C. Kittel, Phys. Rev. 98, 368 (1955).

containing T_2 represents the effect of the degeneracy of valence bands and the term containing T_3 represents the splitting due to the lack of inversion symmetry. Moreover, (2.5) implies that the splittings due to the inversion asymmetry for the otherwise degenerate bands are equal amount in the opposite directions. Except for a few cases, such as beating effect in Shubnikov–de Haas oscillations, the effect of the inversion asymmetry splitting might be ignored. We will, therefore, consider only the energy band averaged over the two bands split due to inversion asymmetry. The inversion asymmetry splitting and the corresponding beating effect will be treated separately.

It is more convenient to express the factor T_2 given in (2.6) in terms of the Kubic harmonics as

$$T_2=\frac{1}{5}-\frac{2}{5(21)^{1/2}}K_{4,1}. \tag{2.8}$$

We thus represent the band averaged over the two split bands in the form

$$E(\mathbf{k})=E_0+(E_2^{(1)}+E_2^{(2)}K_{4,1})k^2+(E_4^{(1)}+E_4^{(2)}K_{4,1})k^4 +(E_6^{(1)}+E_6^{(2)}K_{4,1}+E_6^{(3)}K_{6,1})k^6 \tag{2.9}$$

for the purpose of analyzing the Fermi surface and effective mass associated with the Γ point.

We represent the inversion asymmetry splitting $\Delta E(\mathbf{k})$ by

$$\Delta E(\mathbf{k})=E_3T_3k^3, \tag{2.10}$$

as given in (2.5). This form of the inversion asymmetry splitting was first derived by Dresselhaus.[17] It should be possible to improve the representation of $E(\mathbf{k})$ by developing higher-order terms in $\mathbf{k}\cdot\mathbf{p}$ theory. These would be especially desirable for the heavy-hole band for which the representation (2.10) is not quite satisfactory. It is found that this splitting in other bands is reasonably well represented by (2.10). As a result, the inversion asymmetry splitting for a band is represented by a single parameter E_3.

To determine the coefficients $E_2^{(1)}$, $E_2^{(2)}$, $E_4^{(1)}$, $E_4^{(2)}$, $E_6^{(1)}$, $E_6^{(2)}$, $E_6^{(3)}$, and E_3 from the calculated energy bands near $\mathbf{k}=0$, we have used a weighted least-squares procedure. We calculated the energy levels at 21 different $\mathbf{k}$ points in the neighborhood of Γ point by the method described in Ref. 12. We then obtained the levels averaged over the pairs of split bands for the conduction, heavy-hole, light-hole, and split-off bands. Using these values, we determined the coefficients in (2.9) by a weighted least-squares procedure. The weights in this least-squares procedure were provided in such a way that the values

$$\sum_{j=1}^{21}[E_0(\mathbf{k}_j)-E(\mathbf{k}_j)]^2/[E_0(\mathbf{k}_j)]^2$$

should be minimized, where $E_0(\mathbf{k}_j)$ and $E(\mathbf{k}_j)$ are the energy values obtained by the band calculation and by the representation (2.9), respectively. The values for E_3 are evaluated using a similar weighted least-squares fit for the values of $\Delta E(\mathbf{k})$.

The determined coefficients of the representation (2.9) and (2.10) are listed in Table I for all the bands considered. The values of $\mathbf{k}$ used in the expansion (2.9) and (2.10) are $10\times(a/2\pi)$ times those of $\mathbf{k}$ given in atomic units (a being the lattice parameter in atomic units). The values of the energy in these representations are given in the unit of electron volts. To convert the coefficients $E_n^{(1)}$, $E_n^{(2)}$, $E_n^{(3)}$, etc., with $n=2, 3, 4, \ldots$, into atomic units (both in energy and $\mathbf{k}$ vector), it is necessary to multiply them by a factor $\alpha^n/13.605$, where α is $10\times(a/2\pi)=18.333$. The largest disagreement between the energy values evaluated by (2.9) and those obtained by the energy-band calculation is about 0.05% for the conduction band. Similar accuracy was obtained for the representations of valence bands.

TABLE I. Coefficients of the energy expansion given by (2.9) and (2.10). The values of $\mathbf{k}$ used in this expansion are $10\times(a/2\pi)$ times those of $\mathbf{k}$ in atomic units. The energy values in this expansion are given in electron volts.

	Conduction band	Heavy-hole band	Light-hole band	Split-off band
$E_2^{(1)}$	1.0239620	0.0734897	0.9122749	0.2403520
$E_2^{(2)}$	0.0	0.0202314	−0.0247716	0.0
$E_4^{(1)}$	−1.1320772	0.0837259	−0.9878922	0.2908739
$E_4^{(2)}$	0.0565828	0.0599069	0.0507158	−0.0545411
$E_6^{(1)}$	1.1072073	−0.2936364	0.5229867	−0.7823455
$E_6^{(2)}$	−0.1134024	−0.2707260	0.0903271	0.2818397
$E_6^{(3)}$	−0.0072275	−0.0262378	−0.0654968	−0.0407913
E_3	0.0469192	0.0023783	0.0900835	0.0398402

From this table, we observe that the inversion asymmetry splittings are largest for the light-hole band, relatively moderate for the conduction and split-off bands, and least for the heavy-hole band. The single-parameter representation of (2.10) for these splittings is generally satisfactory (the largest disagreement being about 10%), except for the heavy-hole band whose inversion asymmetry splitting vanishes according to Kane's $\mathbf{k}\cdot\mathbf{p}$ theory. The absolute magnitude of these splitting for the heavy-hole band is so small that the discrepancy in its representation is not significant. (For the heavy-hole band, the coefficient E_3 is obtained by the ordinary least-squares procedure rather than the weighted least-squares procedure.) In general, the representations of the bands by (2.9) and (2.10) are satisfactorily precise within a reasonable range of $\mathbf{k}$ space around $\mathbf{k}=0$. We make the analysis of the bands using these representations in the following sections.

To the lowest order in the $\mathbf{k}\cdot\mathbf{p}$ analysis, the valence bands can be represented by

$$E(\mathbf{k})_{\pm}=Ak^2\pm[B^2+C^2T_2]k^2, \tag{2.11}$$

where + and − correspond to the heavy-hole and

[17] G. Dresselhaus, Phys. Rev. 100, 580 (1955).

light-hole bands, respectively. The usual band-edge parameters L, M, N, and also F, G, H, are related to the parameters A, B, and C.[16] From (2.9) and (2.11), we obtain the relations

$$E_2^{(1)}=A\pm(B^2+C^2/5)^{1/2},$$
$$E_2^{(2)}=\mp C^2/\{5(21)^{1/2}(B^2+C^2/5)^{1/2}\}$$

assuming

$$2C^2K_{4,1}/\{5(21)^{1/2}(B^2+C^2/5)\}\ll 1.$$

From these relations, we determined (in atomic units)

$$A=-12.18,\quad |B|=9.00,\quad |C|=11.49.$$

Alternatively, the values of A, B, and C can be determined from (2.11) using a least-squares procedure; indeed, it is found that the values determined by this way converge to the above values as we take the magnitude of $\mathbf{k}$ values smaller.

III. FERMI SURFACE AND INVERSION-ASYMMETRY EFFECT

Many interesting magnetic effects occurring in n-type doped GaSb are due to the periodic changes in the density of states of the conduction electrons as the applied magnetic field is varied. The oscillations in the magnetoresistance in this material are investigated for the samples with various range of Fermi levels.[1–3,6] Similar oscillations in the Hall coefficient are also observed for this material and it is found that the periods of oscillations for these two effects are in very close agreement with each other.[2]

The period P and the frequency F of this kind of oscillation, which are induced by the magnetic quantization of levels, is related to the extremal cross-sectional area A of the Fermi surface perpendicular to the applied magnetic field by

$$P=1/F=2\pi e/\hbar A \tag{3.1}$$

in mks units. We can obtain the Fermi-level dependence and anisotropy of the period of the oscillation by evaluating the extremal cross-sectional areas as functions of Fermi level in various directions.

The extremal cross-sectional area $A(E_F)$ is obtained by

$$A(E_F)=\tfrac{1}{2}\int_0^{2\pi} k_F^2(E_F,\theta)d\theta, \tag{3.2}$$

where $k_F(E_F,\theta)$ is the value of $\mathbf{k}$ vector on the Fermi surface and the integral is performed on the surface perpendicular to the applied magnetic field. In the present investigation, we consider the cross-sectional area associated with three major directions of symmetry of magnetic field: ⟨100⟩, ⟨110⟩, and ⟨111⟩.

From (2.9), the Fermi level E_F is given by

$$Z=(1+\mu K_{1,4})k_F^2+(\alpha+\beta K_{4,1})k_F^4+(\gamma+\delta K_{4,1}+\epsilon K_{6,1})k_F^6, \tag{3.3}$$

where

$$Z=(E_F-E_0)/E_2^{(1)},$$
$$\alpha=E_4^{(1)}/E_2^{(1)},\quad \beta=E_4^{(2)}/E_2^{(1)},\quad \gamma=E_6^{(1)}/E_2^{(1)},$$
$$\delta=E_6^{(2)}/E_2^{(1)},\quad \epsilon=E_6^{(3)}/E_2^{(1)},\quad \mu=E_2^{(2)}/E_2^{(1)}.$$

Inverting (3.3), we obtain

$$k_F^2=Z\left\{\frac{1}{1+\mu K_{4,1}}-Z\frac{\alpha+\beta K_{4,1}}{(1+\mu K_{4,1})^3}+Z^2\left[\frac{2(\alpha+\beta K_{4,1})^2}{(1+\mu K_{4,1})^5}-\frac{\gamma+\delta K_{4,1}+\epsilon K_{6,1}}{(1+\mu K_{4,1})^4}\right]\right\}. \tag{3.4}$$

Since $\mu=0$ for the conduction band, we can reduce it to the form

$$k_F^2=F_1(Z)+F_2(Z)K_{4,1}+F_3(Z)K_{6,1}+F_4(Z)K_{4,1}^2, \tag{3.5}$$

where

$$F_1(Z)=Z-\alpha Z^2+(2\alpha^2-\gamma)Z^3,$$
$$F_2(Z)=-\beta Z^2+(4\alpha\beta-\delta)Z^3,$$
$$F_3(Z)=-\epsilon Z^3,$$
$$F_4(Z)=2\beta^2Z^3.$$

We then easily perform the integral in (3.2) on the surfaces perpendicular to the ⟨100⟩, ⟨110⟩, and ⟨111⟩ directions.

The calculated frequency versus Fermi energy curves obtained from (3.2) and (3.1) are given in Fig. 1. In

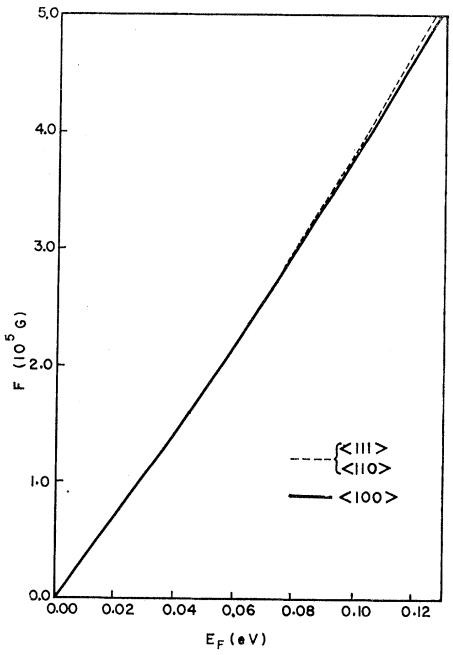

FIG. 1. Frequency versus Fermi energy for conduction band. The solid line represents the ⟨100⟩ direction and the dashed line represents the ⟨111⟩ and ⟨110⟩ directions. The values of frequency in the ⟨111⟩ and ⟨110⟩ directions are nearly identical and therefore are not shown separately.

TABLE II. A comparison between the calculated and measured periods of the Hall coefficient and magnetoresistance oscillations. P_c represents the calculated periods, and P_R and P_ρ represent the measured periods of the Hall coefficient and magnetoresistance oscillations, respectively. E_F is the Fermi energy of the measured sample. The experimental data are taken from Ref. 2.

	Experimental		Calculated		
E_F (eV)	P_R (10^{-6} G^{-1})	P_ρ (10^{-6} G^{-1})	P_c (10^{-6} G^{-1})		
			⟨100⟩	⟨110⟩	⟨111⟩
0.1048	2.51	2.49	2.493	2.474	2.470
0.0954	2.80	2.73	2.768	2.749	2.744
0.0937	2.83	2.81	2.823	2.804	2.800
0.0907	2.94	2.89	2.927	2.908	2.903
0.0895	2.99	2.93	2.970	2.951	2.947
0.0779	3.44	3.42	3.457	3.438	3.434
0.0531	5.49	5.57	5.213	5.195	5.191
0.0484	6.09	5.98	5.748	5.731	5.727

Table II, we have made a comparison between the calculated and measured periods of the Hall coefficient and magnetoresistance oscillations for a number of samples with different Fermi levels. The experimental data listed in this table are obtained from Ref. 2. For most of the samples, the calculated periods are in excellent agreement with measured values.

Next, we present a comparison between the theory and experiment for the anisotropy of the frequencies of the magnetoresistance oscillations. In Table III, the frequencies of the magnetoresistance oscillations measured by Seiler and Becker[6] with the magnetic field in the ⟨100⟩, ⟨110⟩, and ⟨111⟩ directions are listed together with the corresponding calculated values. Since the Fermi levels of the samples used in these measurements are not explicitly given by the authors, we made the comparison with the calculated values which make exact agreement with the experimental data in ⟨111⟩ direction. By doing this, we can make the most clear comparison for the anisotropy of the frequencies. The Fermi levels, at which the calculated values were taken, are also given in the table.

The result of the present calculation, which is directly obtained from an energy-band calculation, explains the measured angular variation very successfully. A similar result has been obtained by Seiler and Becker,[6] who included only $K_{4,1}$ type anisotropy. The relative amount of contribution from $K_{6,1}$ term is small compared with that of $K_{4,1}$. (See Table I for the corresponding coefficients.)

TABLE III. Anisotropy of the frequencies of the magnetoresistance oscillations. The experimental data are taken from Ref. 6. The unit of the frequency is 10^5 G.

Fermi energy	Direction	Experimental[a]	Calculated
0.0956	⟨111⟩	3.649	3.649
	⟨110⟩	3.643	3.643
	⟨100⟩	3.617	3.617
0.1048	⟨111⟩	4.048	4.048
	⟨110⟩	4.043	4.041
	⟨100⟩	4.008	4.010

[a] Seiler remeasured these values recently and obtained slightly different values [D. G. Seiler (private communication)].

We estimate the distance between two successive nodes of the beat patterns caused by the inversion asymmetry splitting in the extremal cross-sectional area of the Fermi surface. In the present calculation, we neglect the possible effects of the interaction between the electronic spin and applied magnetic field.

For the case in which the magnetic field is in either the ⟨100⟩ or ⟨110⟩ direction, some complication arises in distinguishing the proper cross-sectional areas split due to inversion asymmetry because the Fermi surfaces for these two split levels touch each other in ⟨100⟩ and ⟨111⟩ axes. Some detailed study has been made for these complicated cases by Roth *et al.*[5] We here consider only the case in which the magnetic field is in a ⟨111⟩ direction. In this case no such complication arises because there are two unambiguously distinct cross-sectional areas.

The difference between these two cross-sectional areas is obtained by

$$\Delta A(Z)=-2Z^{3/2}\int_0^{2\pi} W d\theta+3Z^2\int_0^{2\pi} W^2 d\theta +\tfrac{1}{4}Z^{5/2}\int_0^{2\pi}(28UW-21W^3)d\theta +10Z^3\int_0^{2\pi}(W^4-2UW^2)d\theta, \quad (3.6)$$

where

$$U=\alpha+\beta K_{4,1}, \quad W=(E_3/E_2^{(1)})T_3.$$

At the Fermi energy of experimental range, the first

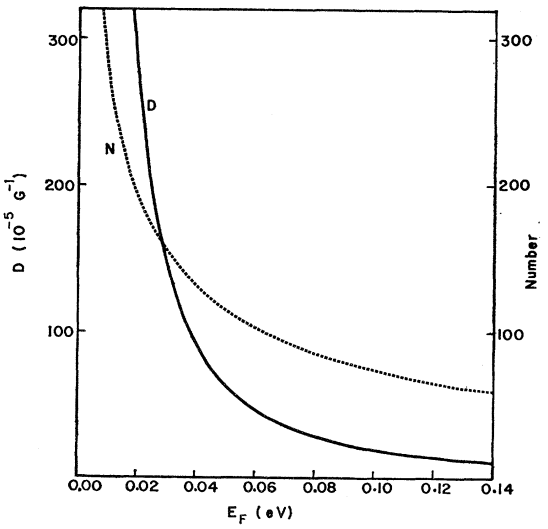

FIG. 2. Distance and number of oscillations between two successive nodes of beat pattern in Shubnikov–de Haas oscillations. Solid line represents the distance between two successive nodes in the unit of 10^{-5} G^{-1} and the dashed line represents the number of oscillations between them.

term and the third term in (3.6) contribute about 70 and 30%, respectively. The contribution from the other terms are order of 1%. The integrands in (3.6) are complicated functions of angle and therefore we performed the integrals numerically. The calculated distance and the number of oscillations between two successive nodes are given in Fig. 2 as functions of Fermi level.

The experimentally observed distance between two successive nodes in the beat pattern reported by Seiler and Becker is 11.7×10^{-5} G^{-1} for the sample with the estimated Fermi level 0.105 eV. From Fig. 2, we observe that the corresponding theoretical value is 17.7×10^{-5} G^{-1}. Although the agreement is poor quantitatively, it provides a strong evidence for the fact that the beating effect is arising from the inversion asymmetry splitting, as proposed by Roth *et al.*[5] More intensive theoretical investigations including the interaction between the electronic spin and external magnetic field, as performed by Roth *et al.*[5] for HgSe, will be necessary to account for the beat patterns in GaSb more satisfactorily. Roth's calculation shows that there is a serious departure from the classical result due to the magnetic-breakdown effect.

IV. EFFECTIVE MASSES

The effective mass m^* related to the cyclotron resonance is given by

$$m^*=(\hbar^2/2\pi)[dA(E_F)/dE_F], \tag{4.1}$$

where E_F is the Fermi energy and $A(E_F)$ is the extremal cross-sectional area of the Fermi surface perpendicular to the applied magnetic field. In atomic units, we rewrite it as

$$\frac{m^*}{m_0}=\frac{1}{\pi}\frac{dA(E_F)}{dE_F}=\frac{1}{2\pi}\int_0^{2\pi}\frac{k_F^2(E_F,\theta)}{dE_F}d\theta, \tag{4.2}$$

where m_0 is the electronic mass and $k_F(E_F,\theta)$ is the value of $\mathbf{k}$ vector on the Fermi surface. We have already expressed k_F^2 in (3.4) in terms of Fermi energy and Kubic harmonics. The integral in (4.2) can be evaluated using k_F^2 given in (3.5) for the conduction and split-off bands using the condition $\mu=0$. For the heavy-hole and light-hole bands, this condition is no longer true and we have to evaluate the integral numerically. The calculated effective-mass–versus–Fermi-energy curves are given in Figs. 3–5 for the conduction, heavy-hole, and light-hole bands. The values of the Fermi energy at the minimum (or maximum) of the corresponding bands

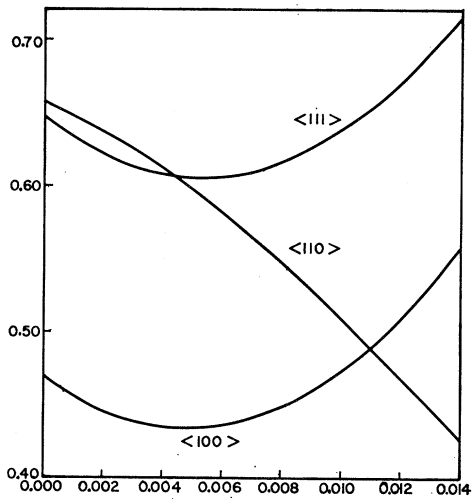

FIG. 4. Effective mass versus Fermi energy for heavy-hole band.

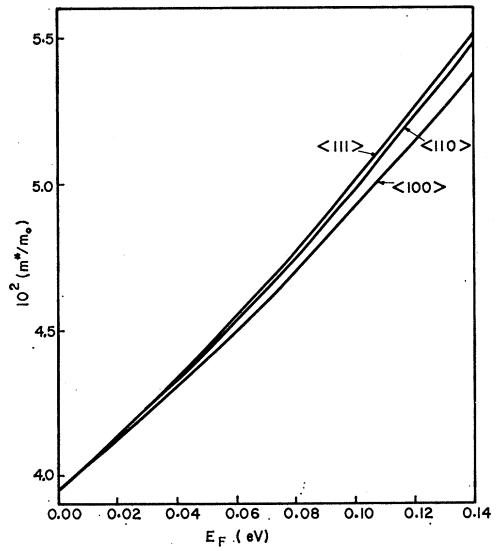

FIG. 3. Effective mass versus Fermi energy for conduction band.

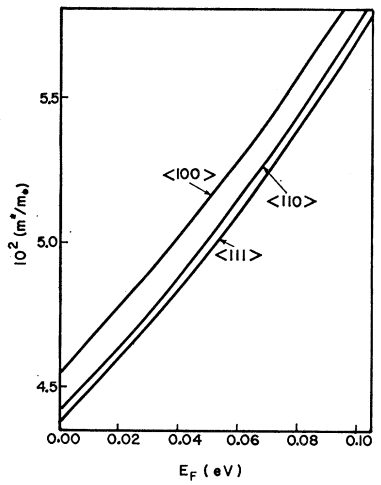

FIG. 5. Effective mass versus Fermi energy for light-hole band.

are taken to be zero. The Fermi-energy values of the valence bands are also taken to be positive.

To obtain the carrier-concentration dependence of the effective mass, we need to find the carrier concentration as a function of Fermi energy. The carrier concentration occupying states near $\mathbf{k}=0$ is given by

$$\rho(E_F)=\frac{2}{(2\pi)^3}\int_{E_F} d^3k=\frac{1}{12\pi^3}\int k_F{}^3 d\Omega. \quad (4.3)$$

For the conduction band, we can easily obtain the expression $k_F{}^3$ from (3.5) which contains only polynomials up to second order of Kubic harmonics for the angular part. Making use of the orthonomality of Kubic harmonics, we can obtain the carrier concentration as a function of Fermi level even without performing actual integrations.

For the conduction band, as the Fermi level crosses over the energy of L minima, the states near L points begin to be occupied. We assume that the energy surfaces in the vicinity of L points are ellipsoidal and thus obtain an expression for the concentration of carriers occupying the states near L minima:

$$\rho_L(E_F)=\frac{4}{3\pi}(E_F-E_L)^{3/2}m_t\sqrt{m_l}. \quad (4.4)$$

E_L is the energy level at L point and m_l and m_t are longitudinal and tangential effective mass associated with L point. In our calculation, we have used the results obtained in a previous work[18] for these values. The carrier concentration of electrons for the Fermi energy higher than E_L is expressed as a sum of (4.3) and (4.4).

The calculation of the carrier concentration for holes is more complicated because of the term containing μ. Only a rough estimate is made for hole concentration as a function of Fermi level for p-type GaSb.

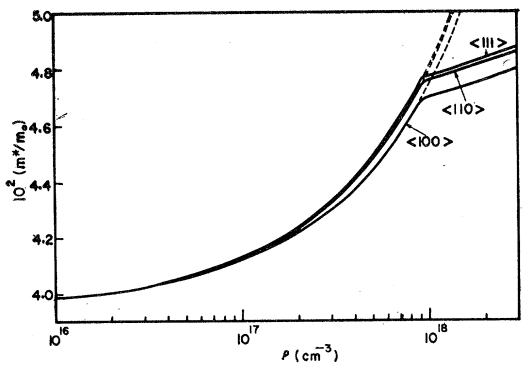

FIG. 6. Effective mass versus carrier concentration for conduction band. Dashed lines represent the case in which the effect of L minima is neglected.

[18] H. I. Zhang and J. Callaway, Solid State Commun. 6, 515 (1968).

The calculated conduction-band effective mass as a function of conduction-electron concentration is given in Fig. 6.

The calculated cyclotron-resonance effective mass for the conduction band makes a reasonable agreement with experiment both in Fermi-energy dependence and anisotropy. In Table IV, a comparison is made between calculated and experimentally measured values of conduction-band effective mass. The set of the experimental values cited in this table is a collection of values measured by a number of different investigators with different methods. Therefore, it is not possible to extract the precise Fermi-energy dependence of the effective mass from these experimental data. In this table, we present the values of effective mass calculated in three different directions.

The calculated anisotropy of the conduction-band effective mass is compared with a measurement by

TABLE IV. Comparison of calculated masses with experimentally measured values for conduction band.

Fermi energy[a] (eV)	Effective mass ($10^2\ m^*/m_0$) Expt.	Calc. ⟨100⟩	⟨110⟩	⟨111⟩
0.031	4.2±0.6[b]	4.218	4.235	4.239
0.035	3.9±0.4, 4.1±0.6[b]	4.254	4.274	4.279
0.044	3.9±0.5[b]	4.337	4.364	4.371
0.046	4.9±0.5[c]	4.356	4.385	4.391
0.050	4.4±0.6, 4.3±0.3[b]	4.394	4.426	4.433
0.067	4.7±0.3[d]	4.561	4.606	4.617
0.080	5.2±0.2[e]	4.694	4.750	4.763

[a] Values of Fermi energy are taken from Ref. 8.
[b] Reference 8.
[c] H. Piller, J. Chem. Phys. Solids 24, 425 (1963).
[d] S. Zwerdling, B. Lax, K. Button, and L. M. Roth, J. Phys. Chem. Solids 9, 320 (1959).
[e] W. M. Becker, A. K. Ramdas, and H. Y. Fan, J. Appl. Phys. Suppl. 32, 2094 (1961).

Seiler and Becker[6] in Table V. Since the correlation between the effective mass and Fermi energy is not uniquely given in their experiment, we compare the experimental values of effective mass with calculated ones which would make exact agreement in ⟨100⟩ directions. From this comparison, we find that the agreement with experiment is reasonable for the anisotropy of the conduction-band effective mass.

For the heavy-hole effective mass, we find only a qualitative agreement with experiment. The absolute values of the heavy-hole mass turned out to be significantly larger than the values measured by Stradling.[9] However, a remarkable agreement is found in the anisotropy. A comparison between calculated heavy-hole mass (for the estimated hole concentration $\sim 10^{18}$ cm^{-3}) and the experimental values of Stradling is given in Table VI. Although both heavy-hole mass and light-hole mass are sensitive to the Fermi level, they are not very sensitive to the hole concentration due to the large density of states in the valence bands. The

TABLE V. Anisotropy of conduction-band effective mass. The experimental values are taken from Ref. 6.

Direction	Experimental m^*/m_0 in units of 10^2	Calculated m^*/m in units of 10^2
⟨100⟩	4.66±0.08	4.660
⟨110⟩	4.69±0.06	4.714
⟨111⟩	4.74±0.07	4.726

light-hole mass shows a stronger degree of anisotropy than the conduction-band effective mass but not as strong as that of the heavy-hole mass. The calculated magnitude of the light-hole mass is found to be a little smaller than the measured value $0.052m_0$ of Stradling.[9] Stradling did not observe any anisotropy of light-hole mass in his measurements in three different directions, but the calculated anisotropy is within the range of uncertainty of his measurement.

The Fermi-energy dependence of the split-off band effective mass does not have much physical significance because it is very unlikely for a significant number of holes to occupy states in this band to form a meaningful Fermi level. (The Fermi level in this context is defined only for the holes occupying this band.) Since the top of this band locates at the level about 0.8 eV lower than the top of other valence bands, the effective mass in the split-off band is virtually independent of the hole concentration. The calculated value of the split-off band mass shows a slight anisotropy, and the magnitude of this mass about $0.17m_0$ coincides with the calculated value for this by Higginbotham *et al.*[19] There is no available experimental information for the value of the split-off band mass.

TABLE VI. Comparison of calculated heavy-hole masses with experimental values. The experimental values are taken from Ref. 9.

Direction	Experimental m^*/m_0	Calculated m^*/m_0
⟨111⟩	0.36±0.03	0.606
⟨110⟩	0.36±0.03, 0.38±0.03	0.598
⟨100⟩	0.26±0.04	0.435

V. CONCLUSION

We have constructed a convenient and realistic representation of energy band which is valid in a substantial region of the Brillouin zone around $\mathbf{k}=0$. Many interesting physical effects in a semiconductor, whose conduction-band minimum is located at $\mathbf{k}=0$, can be accounted for by the energy bands in this region. Previously, only $\mathbf{k}\cdot\mathbf{p}$ perturbation theory supplied the theoretical explanation for them, but because of the absence of the higher-order terms than k^2, the validity of this theory is restricted. Our representation of the energy band, which has wider validity than the $\mathbf{k}\cdot\mathbf{p}$ representation, is directly related to our previous energy-band calculation for GaSb.

A detailed analysis has been made for the Fermi surface and effective mass of the conduction band using this band representation. Most of the calculated results agree with experiment quite satisfactorily. This gives an additional justification for our previous band calculation. More detailed study is desirable for the explanation of the beating effect observed in GaSb using our band representation. Some disagreement is found between the calculated and measured effective masses for the valence bands. More experimental and theoretical investigations seem to be needed to obtain clearer picture of the valence bands.

ACKNOWLEDGMENTS

The author wishes to express his sincere gratitude to Professor J. Callaway, whose guidance made this work possible. He is also grateful to Dr. M. Okazaki for helpful discussions. The author is indebted to Dr. D. G. Seiler and Dr. W. M. Becker for communication of their results prior to publication.

[19] C. W. Higginbotham, F. H. Pollak, and M. Cardona, in Proceedings of the International Conference on the Physics of Semiconductors, Moscow (to be published).